1 **Intrabacterial regulation of a cytotoxic effector by its cognate metaeffector promotes**

2 ***Legionella pneumophila* virulence**

3

4 Deepika Chauhan,[a]* Ashley M. Joseph,[a] Stephanie R. Shames[a]#

5

6 [a]Division of Biology, Kansas State University, Manhattan, Kansas 66506 USA

7

8 Running title: Intrabacterial effector regulation by a metaeffector

9

10 #Address correspondence to Stephanie R. Shames, sshames@ksu.edu

11

12 *Present address: Department of Diagnostic Medicine and Pathobiology, College of Veterinary

13 Medicine, Kansas State University, Manhattan, Kansas 66506

14

Abstract

Legionella pneumophila is a natural pathogen of unicellular protozoa that can opportunistically infect macrophages and cause Legionnaires' Disease. Intracellular replication is driven by hundreds of bacterial effector proteins that are translocated into infected host cells by a Dot/Icm type IV secretion system. *L. pneumophila* effectors are temporally regulated in part by a unique family of translocated regulatory effectors, termed metaeffectors, which bind and modulate the function of a cognate effector in host cells. We discovered that regulation of the cytotoxic effector SidI by its metaeffector, MesI, is critical for *L. pneumophila* virulence in natural and opportunistic hosts. MesI binds and negatively regulates SidI activity *in vitro* but how dysregulation of SidI impairs *L. pneumophila* intracellular replication is unclear. Using a chromosomally-encoded inducible expression system, we discovered that dysregulation of SidI, via loss of MesI, was toxic to *L. pneumophila.* SidI enzymatic activity was required for toxicity since *L. pneumophila* growth was unaffected by induced expression of a catalytically inactive *sidI* allele. We found MesI translocation into host cells was dispensable for intracellular replication and that MesI-deficient bacteria were rapidly degraded within host cells. Together, our data suggest a unique role for intrabacterial effector regulation by a translocated metaeffector in *L. pneumophila* virulence.

32 **Importance**

33 *Legionella pneumophila* replicates within phagocytic host cells using hundreds of effector protein
34 virulence factors, which canonically subvert the function of host proteins and pathways. *L. pneu-*
35 *mophila* encodes a unique family of translocated effectors called metaeffectors, which bind and
36 regulate the function of a cognate effector in host cells. The metaeffector MesI promotes *L. pneu-*
37 *mophila* virulence by regulating the cytotoxic effector SidI; however, the MesI regulatory mecha-
38 nism is poorly understood. We discovered a unique intrabacterial role for MesI in *L. pneumophila*
39 virulence. When uncoupled from MesI, SidI was toxic to *L. pneumophila in vitro* and triggered
40 robust bacterial degradation in host cells. Importantly, translocation of MesI was dispensable for
41 intracellular replication, demonstrating that intrabacterial regulation of SidI contributes to *L.*
42 *pneumophila* virulence. These data show a unique and important role for MesI regulation of SidI
43 within the bacterium, which challenges the dogma that effectors function exclusively within host
44 cells.

45

46

47 **Introduction**

48 *Legionella pneumophila* is ubiquitous in freshwater environments where it parasitizes and repli-
49 cates within free-living protozoa. Co-evolution with environmental phagotrophs have conferred
50 on *L. pneumophila* the ability to replicate within mammalian macrophages, which results in a se-
51 vere inflammatory pneumonia called Legionnaires' Disease (1–3). Within host cells, *L. pneumoph-*
52 *ila* replicates within an endoplasmic reticulum (ER)-derived compartment called the *Legionella-*
53 containing vacuole (LCV), which avoids endocytic maturation and fusion with lysosomes (4, 5).
54 Biogenesis of the LCV is facilitated through the activity of over 300 effector proteins, bacterial
55 virulence factors translocated into host cells through a Dot/Icm type IV secretion system (T4SS)
56 (6). Dot/Icm-translocated effectors are critical for *L. pneumophila* virulence in natural and oppor-
57 tunistic hosts (7); however, the role of most effectors remains poorly understood due primarily to
58 functional redundancy and rarity of virulence phenotypes in laboratory infection models.

59 Many Gram-negative bacterial pathogens employ effector proteins as part of their virulence
60 strategy. Canonically, effector proteins function by targeting host proteins and subverting cellular
61 pathways to the benefit of the pathogen; however, *L. pneumophila* encodes a unique family of
62 translocated effectors termed metaeffectors, which bind and regulate other *L. pneumophila* effec-
63 tors within host cells (8, 9). Metaeffectors are a key component of *L. pneumophila* pathogenicity
64 since several are required for intracellular replication but how most metaeffectors promote viru-
65 lence is poorly understood.

66 We discovered that regulation of the effector SidI (Lpg2504) by its cognate metaeffector,
67 MesI (Lpg2505), is critical for *L. pneumophila* virulence (10). Like most *L. pneumophila* effectors,
68 loss of SidI has no effect on virulence in laboratory infection models; however, loss-of-function

69 mutation in *mesI* (Δ*mesI*) uniquely attenuates *L. pneumophila* virulence in amoebae, macrophages,
70 and mouse models of Legionnaires' Disease only when SidI is produced (10). SidI is a cytotoxic
71 glycosyl hydrolase that inhibits eukaryotic mRNA translation (11, 12). MesI binds SidI with high
72 affinity, suppresses its toxicity, and blocks SidI-mediated translation inhibition *in vitro* (12). The
73 requirement for MesI is relieved when *sidI* is deleted (Δ*sidI*); however, a single amino acid substi-
74 tution that renders SidI non-toxic and catalytically inactive (R453P) is also sufficient to restore
75 replication of MesI-deficient *L. pneumophila* (10). These data have provided key biochemical in-
76 sights into the MesI regulatory mechanism but how MesI regulation of SidI promotes intracellular
77 replication is still unclear.

78 In this study, we made the surprising discovery that MesI promotes *L. pneumophila* viru-
79 lence by regulating SidI intrabacterially. SidI was toxic to *L. pneumophila* when uncoupled from
80 MesI *in vitro*. We found that MesI translocation was dispensable for *L. pneumophila* intracellular
81 replication and MesI-deficient bacteria are rapidly degraded in host cells. These data suggest a
82 unique and important role for interkingdom effector regulation in *L. pneumophila* virulence.
83

84

85 **Results**

86 **Overexpression of *sidI* impairs *L. pneumophila* growth *in vitro*.** We discovered that the *L. pneu-*
87 *mophila* metaeffector MesI promotes bacterial intracellular replication by regulating its cognate
88 effector SidI (10), but how SidI dysregulation attenuates *L. pneumophila* virulence is unclear. A *L.*
89 *pneumophila* Δ*mesI* mutant is impaired for intracellular replication but virulence is restored by *sidI*
90 chromosomal deletion (Δ*sidI*Δ*mesI*) or catalytic inactivation (*sidI*$_{R453P}$Δ*mesI*). We initially validated
91 that dysregulation of SidI impairs *L. pneumophila* intracellular replication plasmid-based genetic
92 complementation of the Δ*sidI* mutation. We infected primary bone marrow-derived macrophages
93 (BMDMs) from *Nlrc4*$^{-/-}$ mice, which are permissive to flagellated *L. pneumophila* (13, 14). Indeed,
94 induced expression of *sidI* from a complementing plasmid severely attenuated *L. pneumophila*
95 replication within BMDMs (**Fig 1A**). Interestingly, we had to induce *sidI* expression at the time of
96 infection since we were unable to culture *L. pneumophila* Δ*sidI*Δ*mesI* (p*sidI*) on inducing media.
97 Inducible plasmid-based genetic complementation is an established technique to fulfill molecular
98 Koch's postulates and we routinely culture *L. pneumophila* on inducing media (10, 12, 15–17). We
99 hypothesized that overexpression of SidI adversely affects bacterial physiology. Indeed, *L. pneu-*
100 *mophila* harboring p*sidI* was unable to replicate in broth under inducing conditions but not in the
101 absence of induction (**Fig 1B**). Impaired growth resulted from SidI enzymatic activity since in-
102 duced the catalytically inactive *sidI*$_{R453P}$ allele did not affect *L. pneumophila* growth (**Fig 1B**). Our
103 initial interpretation was that dysregulation of SidI does not adversely affect *L. pneumophila* phys-
104 iology since *L. pneumophila* Δ*mesI* is not attenuated for growth *in vitro* (10). However, *sidI* expres-
105 sion in broth grown bacteria is ~ 3-fold lower than expression during intracellular replication (18),

106 which may be insufficient to impair *L. pneumophila* growth. Induced expression of an effector gene
107 has not previously been associated with impaired bacterial growth and these data suggest that
108 SidI enzymatic activity is deleterious to *L. pneumophila* when stoichiometrically uncoupled from
109 MesI.
110
111 **MesI rescues the SidI-mediated growth defect *in vitro*.** MesI suppresses SidI toxicity in yeast
112 (10); thus, we hypothesized that MesI also suppresses SidI toxicity in *L. pneumophila*. To test this
113 hypothesis, we generated *L. pneumophila* strains that enable tightly controlled inducible expres-
114 sion of the *sidI-mesI* locus from its endogenous position in the chromosome. We inserted the *araC-*
115 *araBAD* (araBAD) promoter and an in-frame *3xflag* epitope tag directly upstream of *sidI* in the
116 chromosome of WT, Δ*mesI*, and *sidI*$_{R453P}$Δ*mesI L. pneumophila* strains (**Fig 2A**). Kinetics and abun-
117 dance of 3xFLAG-SidI fusion protein production was consistent between strains and only ob-
118 served under arabinose-inducing conditions (**Fig 2B**). We observed a tightly controlled increase
119 in araBAD-mediated *sidI* expression relative to endogenous levels (**Fig 2C**). The ~4-fold increase
120 in *sidI* expression from the araBAD promoter is more physiologically relevant than the >10-fold
121 increase in expression from the P*tac* promoter (**Fig 2C**) (18). Thus, we have established *L. pneu-*
122 *mophila* strains in which we can control expression of *sidI* and *mesI* in their native stoichiometry
123 and endogenous locus in the chromosome.
124 We leveraged our *L. pneumophila* araBAD strains (**Fig 2A**) to test the hypothesis that stoi-
125 chiometric production of MesI abrogates SidI-mediated growth attenuation. We quantified rep-
126 lication our *L. pneumophila* araBAD strains were under inducing and non-inducing conditions and
127 found that induced expression of *sidI,* but not the inactive *sidI*$_{R453P}$ allele, significantly attenuated

128 bacterial growth only when uncoupled from *mesI* in broth culture (**Fig 3A**) and within BMDMs
129 (**Fig 3B**). Thus, the SidI-mediated growth defect is suppressed by MesI.
130
131 **MesI suppresses SidI intrabacterial toxicity.** SidI impairs *L. pneumophila* growth, but it is unclear
132 whether SidI is bacteriostatic or bactericidal. SidI is toxic to yeast (11); thus, we tested the hypoth-
133 esis that SidI is bactericidal when uncoupled from MesI. *L. pneumophila* araBAD strains (**Fig 2A**)
134 were grown for 24 h under arabinose inducing or non-inducing conditions in broth and viability
135 was evaluated by LIVE/DEAD viability staining and confocal microscopy (**Fig 4**). Very few dead
136 bacteria were observed under non-inducing conditions or when induced *sidI* expression was cou-
137 pled with *mesI* (araBAD-WT) (**Fig 4**). However, significantly more dead bacteria were observed
138 when enzymatically active *sidI* was uncoupled from *mesI* under inducing conditions (**Fig 4**). These
139 data suggest that SidI toxicity is conserved across the kingdoms of life and suppressed by MesI.
140
141 **Intrabacterial regulation of SidI by MesI is sufficient for *L. pneumophila* virulence.** Based on
142 our observation that SidI is toxic to *L. pneumophila* when uncoupled from MesI, we hypothesized
143 that MesI intrabacterial regulation of SidI is sufficient for *L. pneumophila* virulence. We tested this
144 by evaluating whether an intrabacterially-retained MesI mutant could complement the Δ*mesI* mu-
145 tation. We generated an allele of *mesI* lacking 10 amino acids from its extreme carboxy terminus,
146 which are dispensable for SidI binding and contains the putative E-block Dot/Icm translocation
147 signal (19, 20), and cloned it into a complementing plasmid downstream of a *3xflag* epitope tag
148 (p*mesI*$_{\Delta 10}$). We evaluated 3xFLAG-MesIΔ10 translocation using Western blot to visualize its abun-
149 dance in saponin-soluble or -insoluble lysate fractions from *L. pneumophila*-infected cells, a

150 technique routinely used to evaluate effector secretion since saponin solubilizes eukaryotic mem-
151 branes but minimally lyses *L. pneumophila* (21, 22). HEK293 FcγRII cells were infected with anti-
152 body-opsonized *L. pneumophila* harboring either p*mesI* or p*mesI*$_{\Delta 10}$. 3xFLAG-MesIΔ10 was not
153 translocated since it was retained in the insoluble fraction (pellet) and not present in saponin-
154 soluble lysate fractions (**Fig 5A**). As expected, wild-type MesI was secreted into host cells since it
155 was present within saponin-soluble lysate fractions (**Fig 5A**). Isocitrate dehydrogenase (ICDH)
156 and β-actin were used as a bacterial lysis and loading controls, respectively. We also confirmed
157 that MesIΔ10 interacts with SidI since it was retained by SidI on beads similarly to full-length
158 MesI (**Fig S1**).

159 To evaluate a role for intrabacterial SidI regulation by MesI in *L. pneumophila* virulence,
160 we tested whether the *mesI*$_{\Delta 10}$ allele genetically complements that Δ*mesI* mutation. We infected
161 BMDMs and quantified replication of wild-type *L. pneumophila* and Δ*mesI* strains harboring p*mesI*,
162 p*mesI*$_{\Delta 10}$, or empty plasmid vector (pEV). We were able to genetically complement the Δ*mesI* with
163 the *mesI*$_{\Delta 10}$ allele, demonstrating that MesI translocation into host cells is not necessary for *L. pneu-*
164 *mophila* intracellular replication (**Fig 5B**). These data suggest that intrabacterial regulation of SidI
165 by MesI is sufficient for *L. pneumophila* virulence.

166

167 **MesI-deficient bacteria are degraded within host cells.** We found that MesI suppresses intrabac-
168 terial SidI toxicity and that MesI translocation into host cells is dispensable for *L. pneumophila*
169 intracellular replication. Since SidI is also toxic to eukaryotic cells, we initially postulated that the
170 virulence defect associated with loss of MesI results from SidI toxicity in host cells. However, we
171 were unable to detect SidI-mediated cytotoxicity in *L. pneumophila*-infected BMDMs (**Fig S2**) and

172 our new data suggest a potential role for MesI suppression of intrabacterial SidI toxicity in *L.*
173 *pneumophila*'s virulence strategy.

174 Dead and dying bacterial are rapidly degraded within host lysosomes; thus, we rational-
175 ized that MesI-deficient bacteria would be robustly degraded within host cells. Degraded *L. pneu-*
176 *mophila* are easily identified by immunofluorescence microscopy since they have lost their rod
177 shape and appear instead as diffuse puncta when cells are stained with a *Legionella*-specific anti-
178 body (23, 24). Thus, we used immunofluorescence microscopy and blinded scoring to quantify
179 degradation of *L. pneumophila* Δ*mesI* within BMDMs. We infected BMDMs and compared kinetics
180 of *L. pneumophila* Δ*mesI* degradation to virulent *L. pneumophila* and *L. pneumophila* Δ*dotA*, which is
181 unable to evade lysosomal degradation (25). After 1 h of infection, most bacteria retained their
182 rod shape and there were no differences between difference *L. pneumophila* strains; however, at 8
183 h post-infection, significantly more *L. pneumophila* Δ*mesI* were degraded compared to both wild-
184 type and Δ*dotA* control strains (**Fig 6**). It is unlikely that bacterial degradation was accompanied
185 by host cell death since macrophages harboring degraded bacteria had normal nuclear morphol-
186 ogy (**Fig 6**). The robust degradation of *L. pneumophila* Δ*mesI* compared to the avirulent Δ*dotA* strain
187 suggests a mechanism of bacterial attenuation distinct from the inability to subvert endocytic
188 maturation.

189

190 **Discussion**

191 This study supports a unique model whereby the *L. pneumophila* metaeffector MesI drives viru-
192 lence by intrabacterial regulation its cognate effector SidI (**Fig 7**). Several *L. pneumophila* effectors
193 are toxic to eukaryotic cells; however, effector bactericidal activity in *L. pneumophila* has not been

194 previously observed. Furthermore, our data challenge the dogma that metaeffectors promote *L.*
195 *pneumophila* virulence by functioning exclusively within host cells. SidI and MesI bear resem-
196 blance to canonical toxin-antitoxin (TA) and effector-immunity (E-I) pairs (26–28); however, they
197 are distinct since anti-toxin/immunity proteins, by definition, are not secreted(29). This also dis-
198 tinguishes MesI from canonical chaperones, which remain intrabacterial (30). MesI negatively
199 regulates SidI subversion of eukaryotic homeostasis (12) and a role for host cell pathways in the
200 MesI regulatory mechanism cannot be fully excluded (**Fig 7**). However, our data suggest a novel
201 mechanism by which *L. pneumophila* virulence hinges on effector regulation by a metaeffector
202 within the bacterium.
203
204 Interkingdom SidI toxicity suggests that its target is highly conserved between *L. pneumophila* and
205 host cells. SidI is it one of at least seven *L. pneumophila* effectors that subvert host protein synthesis
206 (11, 31), one of the most conserved cellular processes across the kingdoms of life (32). Effector-
207 mediated suppression of host mRNA translation is important for *L. pneumophila*'s acquisition of
208 host-derived amino acids, which are essential for intracellular replication and the main driver of
209 bacterial phase switching within host cells (23, 33). The mechanism by which SidI inhibits protein
210 synthesis is unclear; however, SidI binds eEF1A and likely functions as a mannosyltransferase,
211 so it is tempting to speculate that SidI blocks translation by modifying eEF1A (11, 12). However,
212 the functional significance of eEF1A binding remains unclear since it is unaffected by MesI and
213 insufficient for translation inhibition (11, 12). *L. pneumophila* has evolved strategies to prevent
214 intrabacterial suppression of translation. For example, the effector Lgt1 blocks eukaryotic trans-
215 lation by glycosylating eukaryotic elongation factor (eEF)1A on Ser53, which is conserved in

216 eukaryotes but not the bacterial eEF1A homolog, EF-Tu (34, 35). The mechanistic underpinnings
217 of intrabacterial MesI activity is unclear; however, it is tempting to speculate that MesI may func-
218 tion in part to preserve protein synthesis within the bacterium.
219
220 Recent work has challenged the dogma that bacterial effectors function exclusively within host
221 cells. Hardwidge and colleagues revealed that the effectors NleB and NleC from pathogenic *Esch-*
222 *erichia coli* and SseK1 from *Salmonella enterica* Typhimurium function intrabacterially to confer
223 oxidative stress and methylglyoxal resistance (36–38). Our data suggest that intrabacterial MesI
224 activity confers a fitness advantage on *L. pneumophila* by suppressing intrabacterial SidI activity.
225 However, MesI is produced at later time points than SidI when *L. pneumophila* is grown in broth
226 (19), suggesting that low levels of SidI activity within the bacterium may be beneficial at early
227 stages of the *L. pneumophila* lifecycle. Indeed, there is emerging evidence that bacterial TA pairs
228 can shape pathogen physiology by modulating post-transcriptional gene expression (39). How-
229 ever, this activity must be highly regulated by the antitoxin to prevent toxicity. Thus, it is tempt-
230 ing to speculate that SidI and MesI are an ancient TA pair that have been co-opted by the T4SS to
231 subvert both host and pathogen physiology.
232
233 Our data challenge our initial assumption that MesI promotes *L. pneumophila* intracellular repli-
234 cation by preventing SidI-mediated host cell toxicity. We found no SidI-mediated differences in
235 host cell death and observed that macrophages MesI-deficient bacteria had normal morphology.
236 Interestingly, McCloskey *et al* recently proposed a model whereby MesI negatively regulates SidI
237 translocation into host cells (19). MesI binds the extreme C-terminus of SidI, which encodes the

238 canonical E-block Dot/Icm translocation signal (12, 19, 40). McCloskey *et al.* recently suggested
239 that MesI negatively regulates SidI secretion from *L. pneumophila*. However, SidI secretion was
240 not further attenuated when the relative abundance of MesI was increased (19). Furthermore, we
241 did not detect any MesI-mediated differences in SidI translocation from *L. pneumophila* using an
242 the established adenylate cyclase (CyaA) reporter (12). This discrepancy may be a consequence
243 of differences in experimental conditions. Further investigation is required to define the impact
244 of MesI on SidI translocation and the potential role of this activity in the MesI regulatory mecha-
245 nism and *L. pneumophila* virulence.
246
247 Together, this study revealed a unique role for intrabacterial regulation of a translocated effector
248 by its cognate metaeffector in *L. pneumophila* virulence. Our data, in the context of previously
249 published studies (11, 12), suggest that SidI's target is conserved between host and pathogen.
250 Recent phylogenetic analysis suggests ancient and extensive co-evolution between the order *Le-*
251 *gionellales,* which includes *Legionella* spp., and unicellular eukaryotes (41). Thus, metaeffectors
252 may represent an ancient mechanism evolved by pathogenic bacteria for adaptation to eukaryotic
253 hosts.
254
255 **Materials & Methods**
256 **Bacterial strains, plasmids, primers, and culture conditions.** *Escherichia coli* Top10 (cloning),
257 DH5αλ*pir* (allelic exchange) and BL21 (DE3) (protein production) were maintained at 37˚C in
258 Luria-Bertani (LB) medium supplemented with appropriate antibiotics for plasmid maintenance

259 [50 μg mL^{-1} kanamycin, 25 μg mL^{-1} chloramphenicol, or 100 μg mL^{-1} ampicillin]. Protein produc-
260 tion in *E. coli* BL21 (DE3) was induced with 1 mM isopropyl-β-D-1-thiogalactopyranoside (IPTG).
261 All *Legionella pneumophila* strains in this study were derived from *L. pneumophila* Philadel-
262 phia-1 SRS43 (10) and cultured at 37˚C on charcoal–N (2-acetamido)-2-aminoethanesulfonic acid
263 (ACES)-buffered yeast extract (CYE) supplemented with L-cysteine and ferric pyrophosphate as
264 described previously (42). Single colonies were isolated after 4 days of growth on CYE agar and
265 used to generate 48 h heavy patches of bacteria. Where indicated, liquid cultures were grown
266 from heavy-patched bacteria at 37°C in L-cysteine- and ferric pyrophosphate-supplemented
267 ACES buffered yeast extract broth (AYE) (43). Media were supplemented with 10 μg mL-1 chlo-
268 ramphenicol (plasmid maintenance), 10 μg mL-1 kanamycin (allelic exchange), 1 mM IPTG (P*tac*
269 gene expression), or 06-2% L-arabinose (w/v; paraBAD gene expression).
270 Plasmids and oligonucleotide primers used in this study are listed in **Table 1** and **Table**
271 **2**, respectively.
272
273 **Molecular cloning and strain construction.** *L. pneumophila* gDNA isolated using the Illustra ge-
274 nomicPREP DNA spin kit (GE Healthcare) and used as a template for cloning *sidI* and *mesI* into
275 the indicated plasmid vectors. *sidI* was amplified from *L. pneumophila* gDNA using SidIBamHI-
276 F/SidISphI-R, which includes 60 base-pairs (bp) downstream of the *sidI* open reading frame, and
277 cloned as a BamHI/SphI fragment into pJB1806 (44) or downstream of an in-frame *3xflag* epitope
278 tag in pSN85 (45) to generate pJB1806::*sidI* (p*sidI*) and pSN85::*sidI*. To generate p$sidI_{R453P}$, p*sidI* was
279 mutagenized using site-directed mutagenesis with primer pairs SidIR453P-sense/SidIR453P-
280 asense (10). To generate p*mesI* complementation plasmids, *mesI* and $mesI_{\Delta 10}$ open reading frames

281 were amplified from *L. pneumophila* gDNA using MesIBglII-F/MesISphI-R or MesIBglII-
282 F/MesIΔ10SphI-R primer pairs, respectively, and cloned into pSN85 in-frame with the *3xflag*
283 epitope tag. Ligations were transformed into chemically competent *E. coli* Top10 and sequences
284 confirmed by Sanger sequencing (Eton Biosciences). *L. pneumophila* complementation strains were
285 generated by electroporation of plasmids into competent *L. pneumophila* strains using a BioRad
286 Gene Pulser at 2.4 kV, 200 Ω, and 0.25 μF and plated on CYE supplemented with 10 μg mL^{-1}
287 chloramphenicol.

288 For production of recombinant His_6-Myc-MesIΔ10, *mesI*Δ10 was amplified from *L. pneu-*
289 *mophila* gDNA using MesIT7SalI-F/MesIΔ10NotI-R and cloned as a SalI/NotI fragment into
290 pT7HMT (46) downstream of an in-frame His_6-Myc epitope tag. pT7HMT::*mesI* and pGEX::*sidI*
291 were generated previously (**Table 2**) (12). Ligation reactions were transformed into chemically
292 competent *E. coli* Top10 and sequences were confirmed by Sanger sequencing (Eton Biosciences).

293 The *dotA* open reading was deleted from the *L. pneumophila* chromosome using allelic ex-
294 change, as described (47). To generate a clean in-frame deletion of *dotA*, 5′ and 3′ regions flanking
295 the *dotA* open reading frame (726 bp upstream and 1,012 bp downstream) were amplified using
296 DotAKOSacI-F/DotAKONotI-R and DotAKONotI-F/DotAKOSalI-R to generate SacI/NotI and
297 NotI/SalI fragments which were ligated into SacI/SalI digested pSR47s to generate pSR47s::Δ*dotA*,
298 which was conjugated into *L. pneumophila* SRS43 for selection of double crossover events, as de-
299 scribed. Sequences were confirmed by Sanger sequencing (Eton Biosciences) and the ΔdotA phe-
300 notype was confirmed by comparison the established SRS43 *dotA*::Tn strain (10).

301 For allelic exchange to insert the paraBAD promoter and a *3xflag* epitope tag upstream of
302 *sidI* in the *L. pneumophila* chromosome, overlapping primers were used to generate a fusion

303 construct consisting of 1,000 bp upstream of *sidI* (SidIUTR-F/SidIUTR-R; from *L. pneumophila*
304 gDNA), araBAD promoter [araC-pBAD-F/araC-pBAD-R; from pMRBAD::z-CspGFP (a gift from
305 Dr. Brian McNaughton; Addgene #40730) (48)], and *3xflag* fused to the first 1,200 nucleotides of
306 *sidI* (3FLAG-SidI-F/3FLAG-SidI-R; from pSN85::*sidI*), which was ligated as a SacI/SalI fragment
307 into pSR47s to generate pSR47S::araBAD. Plasmids were transformed into chemically competent
308 *E. coli* DH5αλ*pir* and sequences were confirmed by Sanger sequencing (Eton Biosciences). To gen-
309 erate paraBAD strains, pSR47s::paraBAD was conjugated into *L. pneumophila* SRS43 wild type,
310 Δ*mesI*, and *sidI*$_{R453P}$Δ*mesI* (10) and selection of double crossover events was performed as described
311 (47). Sucrose resistant, kanamycin sensitive colonies were screened by PCR to verify gene inser-
312 tion.
313
314 **Mice.** C57Bl/6 *Nlrc4*$^{-/-}$ mice (a gift from Dr. Craig Roy) have been described (49). In-house colonies
315 were maintained under specific pathogen-free conditions at Kansas State University. Bone mar-
316 row was harvested from 8- to 15-week-old mice as previously described (50). All experiments
317 involving animals were approved by the Kansas State University Institutional Animal Care and
318 Use Committee (IACUC-4501 and -4022) and performed in compliance with the Animal Welfare
319 Act and National Institutes of Health guidelines.
320
321 **Cell culture.** All mammalian cells were grown at 37˚C/5% CO2. HEK293 FcγRII cells (a gift from
322 Dr. Craig Roy) were cultured in Dulbecco's Modified Eagle Medium (DMEM; Gibco) supple-
323 mented with 10% heat-inactivated fetal bovine serum (HIFBS; Biowest) for up to 25 passages.
324 Primary mouse bone marrow-derived macrophages (BMDMs) were differentiated in RPMI

325 supplemented with 20% HIFBS (Biowest) and 15% L-929 conditioned medium (Differentiation
326 media) for 6 days prior to infection, as described (50). Differentiated BMDMs were seeded for
327 infections in RMPI supplemented with 10%HIFBS and 7.5% L-929 conditioned medium (Seeding
328 medium).
329
330 **Macrophage growth curves.** BMDMs were seeded into 24-well tissue culture dishes at 2.5 x 10^5
331 per well one day prior to infection. *L. pneumophila* were cultured on CYE agar and heavy patch-
332 grown bacteria were used to infect BMDMs at a MOI of 1 in triplicates and CFU were enumerated
333 as previously described (10, 15). Fold growth was calculated by normalizing CFU at 24 h, 48 h,
334 and 72 h to internalized bacteria at 1 h post-infection. For genetic complementation, either 1 mM
335 IPTG or 2% L-arabinose (w/v) were added to the media as indicated at the time of infection and
336 maintained throughout.
337
338 ***In vitro* growth curves.** *L. pneumophila* heavy patches were resuspended in fresh AYE broth and
339 sub-cultured for consistent 600 nm optical density (OD_{600}). Cultures were split into triplicate wells
340 of a 96-well round-bottom plate and incubated at 37˚C with continuous orbital shaking using an
341 Agilent BioTek Epoch2 plate reader. OD_{600} from triplicate wells was read every two hours for up
342 to 48 h, as indicated. Plasmids were maintained with chloramphenicol and IPTG (1 mM) or 1%
343 L-arabinose (w/v) were added to the media to induce gene expression as indicated.
344
345 **Quantitative RT-PCR.** *L. pneumophila* strains were grown for 1 or 6 h in AYE broth of incubation
346 with and without arabinose (2%), and total RNA was purified with the Direct-zol RNA miniprep

347 kit with TRI-reagent (Zymo Research) following manufacturer's instructions. RNA samples were
348 treated with DNase (Sigma) before reverse transcription with Superscript III (Invitrogen). Quan-
349 titative RT-PCR was performed using the Invitrogen SuperScript III Platinum SYBR Green One
350 Step qRT-PCR kit. Transcript abundance was quantified using sidIRT-F/sidIRT-R (sidI) and
351 16SRT-F/16SRT-R (16S rRNA) primer pairs on a BioRad CFX96 Real-Time PCR machine. Fold
352 expression (2^ΔΔCt) was calculated by normalizing *sidI* transcript abundance to 16S rRNA and
353 standardizing values to wild-type *L. pneumophila*.
354
355 **Bacterial viability and LIVE/DEAD staining.** *L. pneumophila* paraBAD strains were resuspended
356 in AYE media from a heavy patch (48 h). Strains were grown for 24 h at 37°C in the presence or
357 absence of 0.6% L-arabinose (w/v). Cell viability was quantified using a LIVE/DEAD™ *Bac-*
358 Light™ Bacterial Viability kit according to manufacturer's instructions. Bacteria were stained
359 with 5 μM SYTO9 (live; green) and 10 μM propidium iodide (dead; red) (ThermoFisher) and
360 incubated for 15 min at room temperature in the dark. To determine the baseline threshold for
361 dead cells a negative control was used, where cells were treated with 90% ethanol for 1 h. After
362 staining, cells were washed with sterile water and 5μL of resuspended cells were loaded on a
363 glass slide with a coverslip. Images were acquired at the KSU Division of Biology Microscopy
364 Facility using a Zeiss LSM5 Laser Scanning Confocal Microscope using a 100x oil-immersion ob-
365 jective. Percent dead bacteria was calculated by normalizing dead bacteria (red) to total bacteria
366 using ImageJ software. At least 500 cells were evaluated for each strain and culture condition and
367 the researcher performing the analysis was blinded to sample identity.
368

369 **Western blot.** Protein was boiled in Laemmli Buffer and separated by SDS-PAGE and were trans-
370 ferred to polyvinylidene difluoride (PVDF; Fisher Scientific) membranes using a BioRad wet
371 transfer apparatus. The membranes were incubated with blocking buffer [5% nonfat milk powder
372 dissolved in Tris-buffered saline-0.1% Tween 20 (TBST)] for 30 min. Membranes were incubated
373 with primary antibodies [mouse α-FLAG M2 (1:1000; Sigma); rabbit α-ICDH (1:1,000; Sigma);
374 rabbit α-β-actin (Cell Signaling); rabbit α-Myc TAG mAb (71D10) (1:1,000; Cell Signaling)] at
375 1:1,000 in blocking buffer overnight at 4˚C with rocking and subsequently with HRP-conjugated
376 goat α-rabbit or α-mouse secondary antibodies at 1:5,000 (ThermoFisher) in blocking buffer for 2
377 h at room temperature with rocking. Membranes were washed, incubated with ECL reagent (GE
378 Amersham), and imaged by chemiluminescence using an Azure Biosystems c300 Darkroom Re-
379 placer.
380
381 **Saponin solubilization assay.** HEK293 FcγRII cells (51) were seeded in 10 cm poly-L-lysine-
382 coated tissue culture dishes (4 x 10^6) one day prior to infection. *L. pneumophila* strains were
383 patched from fresh single colonies onto CYE agar supplemented with 10 μg mL^{-1} chlorampheni-
384 col and 1 mM IPTG to induce gene expression. Bacteria were opsonized with α-*L. pneumophila*
385 antibody [1:1,000 (Invitrogen; PA17227)] in DMEM 10%HIFBS supplemented with 1 mM IPTG
386 for 20 min at room temperature (RT) with rotation. Cells were infected with opsonized bacteria
387 at a MOI of 50 in for 2 h in 2 mL DMEM 10%HIFBS supplemented with 1 mM IPTG. Cells were
388 washed 3X with ice-cold PBS to remove extracellular bacteria and lysed for 10 min in 500 μL ice-
389 cold Hank's Balanced Salt Solution (HBSS) supplemented with 0.2% saponin and ProBlock™
390 Gold Mammalian Protease Inhibitor Cocktail (GoldBio). Lysates were treated with RNAse A (10

391 μg mL-1) and DNase I (10 μg mL-1), incubated at RT for 15 min, and centrifuged for 15 min at
392 17,000 r.c.f at 4˚C. Saponin-soluble supernatants were filtered using a 0.22 μM syringe filter and
393 transferred to a fresh 1.5 mL microcentrifuge tube. Saponin-insoluble pellets were resuspended
394 in 50 μL TE buffer (10 mM Tris-HCl, 1 mM EDTA). Fifty microliters of supernatant and pellet
395 fractions were diluted in 3X Laemmeli sample buffer, boiled for 10 min, and the whole sample
396 was loaded into wells of a 1.5 mm 15% SDS-PAGE gel for Western blot.
397
398 **Affinity chromatography.** Affinity chromatography from *E. coli* lysates was performed as de-
399 scribed (12). Briefly, *E. coli* BL21 (DE3) harboring pT7HMT::*mesI*, pT7HMT::*mesI*$_{\Delta 10}$,
400 pGEX6P1::sidI, or pGEX6P1 were grown overnight with shaking at 37˚C overnight and sub-cul-
401 tured at 1:100 in LB media. Sub-cultures were grown for 3 h followed by induction with 1 mM
402 IPTG and growth overnight at 16˚C. Clarified lysates from bacteria producing GST-fusion pro-
403 teins were incubated with pre-equilibrated glutathione magnetic agarose beads (Pierce) for 1h at
404 4˚C with rotation. Beads were washed twice in washing buffer (125 mM Tris-Cl, 150 mM NaCl,
405 1mM DTT, 1 mM EDTA, pH 7.4) and incubated with clarified lysates from bacteria producing
406 His$_6$-Myc fusion proteins at 4˚C for 1 h with rotation. Beads were washed twice in washing buffer
407 transferred to a fresh 1.5 mL microcentrifuge tube and boiled in 25 μM 3X Laemmli Sample buffer.
408 Proteins were separated by SDS-PAGE and visualized using Coomassie brilliant blue or Western
409 Blot, as indicated.
410
411 **Cytotoxicity Assay.** Cytotoxicity was evaluated by quantifying lactate dehydrogenase (LDH) ac-
412 tivity in supernatants of *L. pneumophila*-infected BMDMs. BMDMs were seeded in 24-well tissue

413 culture dishes at $2.5x10^5$ in Seeding medium one day prior to infection. Cells were infected with
414 *L. pneumophila* strains at an MOI of 50 for 1 h, washed 3 times with sterile phosphate-buffered
415 saline ($PBS^{-/-}$), and incubated in seeding media for additional 5 h or 9 h. At the indicated times,
416 plates were centrifuged at 250 r.c.f. and supernatants were transferred to a sterile non-tissue cul-
417 ture treated 96 well plate. For the 1 h timepoint, supernatants were collected from cells without
418 washing. LDH was quantified using the CytoTox™ 96 Non-radioactive Cytotoxicity Assay
419 (Promega) and according to manufacturer's instructions. Absorbance at 490 nm was read on a
420 BioTek Epoch2 microplate reader and percent cytotoxicity was calculated by normalizing absorb-
421 ance values to cells treated with lysis buffer.
422
423 **Quantification of bacterial degradation within macrophages.** BMDMs (1×10^5) were seeded on
424 poly-L-lysine-coated glass coverslips in 24-well tissue culture dishes one day prior to infection.
425 BMDMs were infected in triplicate wells with the indicated *L. pneumophila* strains at an MOI of 30
426 for 1 h or 8 h. For the 8 h timepoint, extracellular bacteria were removed after 1 h by washing
427 coverslips three times in $PBS^{-/-}$ and incubated with fresh media for 7 h. Coverslips were fixed in
428 3.7% paraformaldehyde for 15 min and permeabilized with ice-cold methanol. Coverslips were
429 stained with 1:1,000 rabbit α-*L. pneumophila* primary antibody (Invitrogen; PA17227) and 1:500
430 Alexa488-conjugated goat α-rabbit secondary antibody (ThermoFisher). Nuclei were stained with
431 1:2,000 Hoeshst (ThermoFisher) and coverslips were mounted on slides with ProLong™ Gold
432 Antifade Mountant (Invitrogen). Degraded and in-tact bacteria were scored blind on a Leica
433 DMiL LED inverted epifluorescence microscope (*n*=150 per strain and time point). Representative
434 images were acquired at the KSU College of Veterinary Medicine Confocal Core using a Zeiss

435 LSM 880 inverted confocal microscope and processed using Fiji ImageJ and Adobe Photoshop
436 software.
437
438 **Statistical analysis.** Statistical analysis was performed with GraphPad Prism 9 software using
439 unpaired two-tailed *t*-test with a 95% confidence interval. Unless otherwise indicated, data are
440 presented as mean ± standard deviation (s.d.) and statistical analysis was performed on tripli-
441 cate biological replicates.
442

443 **Acknowledgements**

444 We thank Dr. Craig Roy for providing *Nlrc4*$^{-/-}$ mice. This work was funded by NIH/NIGMS Center
445 for Biomedical Research Excellence Research Project Grants (P20GM130448 and P20113117; to
446 S.R.S.), an NIH/NIGMS Kansas-INBRE Postdoctoral Fellowship (P20GM103418; to D.C.), and
447 start-up funds from Kansas State University.
448

449 **References**

450

451 1. Horwitz MA, Silverstein SC. 1980. Legionnaires' disease bacterium (Legionella pneumophila)
452 multiples intracellularly in human monocytes. J Clin Investigation 66:441–50.

453 2. Park JM, Ghosh S, O'Connor TJ. 2020. Combinatorial selection in amoebal hosts drives the
454 evolution of the human pathogen Legionella pneumophila. Nat Microbiol 1–11.

455 3. Gomez-Valero L, Rusniok C, Carson D, Mondino S, Pérez-Cobas AE, Rolando M, Pasricha S,
456 Reuter S, Demirtas J, Crumbach J, Descorps-Declere S, Hartland EL, Jarraud S, Dougan G,
457 Schroeder GN, Frankel G, Buchrieser C. 2019. More than 18,000 effectors in the Legionella genus
458 genome provide multiple, independent combinations for replication in human cells. Proc Na-
459 tional Acad Sci 116:2265 2273.

460 4. Swanson MS, Isberg RR. 1995. Association of Legionella pneumophila with the macrophage
461 endoplasmic reticulum. Infect Immun 63:3609–3620.

462 5. Horwitz MA. 1983. Formation of a novel phagosome by the Legionnaires' disease bacterium
463 (Legionella pneumophila) in human monocytes. The Journal of experimental medicine 158:1319
464 1331.

465 6. Chauhan D, Shames SR. 2021. Pathogenicity and Virulence of Legionella: Intracellular replica-
466 tion and host response. Virulence 12:1122–1144.

467 7. Berger KH, Isberg RR. 1993. Two distinct defects in intracellular growth complemented by a
468 single genetic locus in Legionella pneumophila. Molecular microbiology 7:7 19.

469 8. Joseph AM, Shames SR. 2021. Affecting the Effectors: Regulation of Legionella pneumophila
470 Effector Function by Metaeffectors. Pathogens 10:108.

471 9. Kubori T, Shinzawa N, Kanuka H, Nagai H. 2010. Legionella metaeffector exploits host pro-
472 teasome to temporally regulate cognate effector. Plos Pathog 6:e1001216.

473 10. Shames SR, Liu L, Havey JC, Schofield WB, Goodman AL, Roy CR. 2017. Multiple Le-
474 gionella pneumophila effector virulence phenotypes revealed through high-throughput analy-
475 sis of targeted mutant libraries. Proc National Acad Sci 63:201708553.

476 11. Shen X, Banga S, Liu Y, Xu L, Gao P, Shamovsky I, Nudler E, Luo Z. 2009. Targeting eEF1A
477 by a Legionella pneumophila effector leads to inhibition of protein synthesis and induction of
478 host stress response. Cell Microbiol 11:911 926.

479 12. Joseph AM, Pohl AE, Ball TJ, Abram TG, Johnson DK, Geisbrecht BV, Shames SR. 2020. The
480 Legionella pneumophila metaeffector Lpg2505 (MesI) regulates SidI-mediated translation inhi-
481 bition and novel glycosyl hydrolase activity. Infect Immun https://doi.org/10.1128/iai.00853-19.

482 13. Ren T, Zamboni DS, Roy CR, Dietrich WF, Vance RE. 2006. Flagellin-deficient Legionella
483 mutants evade caspase-1- and Naip5-mediated macrophage immunity. Plos Pathog 2:e18.

484 14. Molofsky AB, Byrne BG, Whitfield NN, Madigan CA, Fuse ET, Tateda K, Swanson MS. 2006.
485 Cytosolic recognition of flagellin by mouse macrophages restricts Legionella pneumophila in-
486 fection. J Exp Medicine 203:1093 1104.

487 15. Ngwaga T, Hydock AJ, Ganesan S, Shames SR. 2019. Potentiation of Cytokine-Mediated Re-
488 striction of Legionella Intracellular Replication by a Dot/Icm-Translocated Effector. J Bacteriol
489 201:13.

490 16. Falkow S. 2004. Molecular Koch's postulates applied to bacterial pathogenicity — a personal
491 recollection 15 years later. Nat Rev Microbiol 2:67–72.

492 17. Falkow S. 1988. Molecular Koch's Postulates Applied to Microbial Pathogenicity. Clin Infect
493 Dis 10:S274–S276.

494 18. Faucher SP, Mueller CA, Shuman HA. 2011. Legionella Pneumophila Transcriptome during
495 Intracellular Multiplication in Human Macrophages. Front Microbiol 2:60.

496 19. McCloskey A, Perri K, Chen T, Han A, Luo Z-Q. 2021. The metaeffector MesI regulates the
497 activity of the Legionella effector SidI through direct protein-protein interactions. Microbes In-
498 fect 104794.

499 20. Burstein D, Zusman T, Degtyar E, Viner R, Segal G, Pupko T. 2009. Genome-Scale Identifica-
500 tion of Legionella pneumophila Effectors Using a Machine Learning Approach. Plos Pathog
501 5:e1000508.

502 21. Puvar K, Iyer S, Fu J, Kenny S, Terón KIN, Luo Z-Q, Brzovic PS, Klevit RE, Das C. 2020. Le-
503 gionella effector MavC targets the Ube2N~Ub conjugate for noncanonical ubiquitination. Nat
504 Commun 11:2365.

505 22. Liu Y, Luo Z-Q. 2007. The Legionella pneumophila effector SidJ is required for efficient re-
506 cruitment of endoplasmic reticulum proteins to the bacterial phagosome. Infect Immun 75:592
507 603.

508 23. Dalebroux ZD, Edwards RL, Swanson MS. 2009. SpoT governs Legionella pneumophila dif-
509 ferentiation in host macrophages. Mol Microbiol 71:640 658.

510 24. Creasey EA, Isberg RR. 2012. The protein SdhA maintains the integrity of the Legionella-
511 containing vacuole. Proc National Acad Sci 109:3481 3486.

512 25. Roy CR, Berger KH, Isberg RR. 1998. Legionella pneumophila DotA protein is required for
513 early phagosome trafficking decisions that occur within minutes of bacterial uptake. Mol Micro-
514 biol 28:663–674.

515 26. Benz J, Meinhart A. 2014. Antibacterial effector/immunity systems: it's just the tip of the ice-
516 berg. Curr Opin Microbiol 17:1–10.

517 27. Altindis E, Dong T, Catalano C, Mekalanos J. 2015. Secretome Analysis of Vibrio cholerae
518 Type VI Secretion System Reveals a New Effector-Immunity Pair. Mbio 6:e00075-15.

519 28. Kirchberger PC, Unterweger D, Provenzano D, Pukatzki S, Boucher Y. 2017. Sequential dis-
520 placement of Type VI Secretion System effector genes leads to evolution of diverse immunity
521 gene arrays in Vibrio cholerae. Sci Rep-uk 7:45133.

522 29. Yang X, Long M, Shen X. 2018. Effector–Immunity Pairs Provide the T6SS Nanomachine its
523 Offensive and Defensive Capabilities. Molecules 23:1009.

524 30. Feldman MF, Cornelis GR. 2003. The multitalented type III chaperones: all you can do with
525 15 kDa. Fems Microbiol Lett 219:151–158.

526 31. Belyi Y. 2020. Targeting Eukaryotic mRNA Translation by Legionella pneumophila. Fron-
527 tiers Mol Biosci 7:80.

528 32. Ganoza MC, Kiel MC, Aoki H. 2002. Evolutionary Conservation of Reactions in Translation.
529 Microbiol Mol Biol R 66:460–485.

530 33. Leon JAD, Qiu J, Nicolai CJ, Counihan JL, Barry KC, Xu L, Lawrence RE, Castellano BM,
531 Zoncu R, Nomura DK, Luo Z-Q, Vance RE. 2017. Positive and Negative Regulation of the Mas-
532 ter Metabolic Regulator mTORC1 by Two Families of Legionella pneumophila Effectors. Cell
533 Reports 21:2031–2038.

534 34. Belyi Y, Tartakovskaya D, Tais A, Fitzke E, Tzivelekidis T, Jank T, Rospert S, Aktories K.
535 2012. Elongation Factor 1A Is the Target of Growth Inhibition in Yeast Caused by Legionella
536 pneumophila Glucosyltransferase Lgt1. J Biol Chem 287:26029 26037.

537 35. Belyi Y, Tabakova I, Stahl M, Aktories K. 2008. Lgt: a family of cytotoxic glucosyltransferases
538 produced by Legionella pneumophila. J Bacteriol 190:3026 3035.

539 36. Qaidi SE, Scott NE, Hardwidge PR. 2021. Arginine glycosylation enhances methylglyoxal
540 detoxification. Sci Rep-uk 11:3834.

541 37. Qaidi SE, Scott NE, Hays MP, Geisbrecht BV, Watkins S, Hardwidge PR. 2020. An intra-bac-
542 terial activity for a T3SS effector. Sci Rep-uk 10:1073.

543 38. Hasan MK, Qaidi SE, Hardwidge PR. 2021. The T3SS Effector Protease NleC Is Active within
544 Citrobacter rodentium. Pathogens 10:589.

545 39. Bertram R, Schuster CF. 2014. Post-transcriptional regulation of gene expression in bacterial
546 pathogens by toxin-antitoxin systems. Front Cell Infect Mi 4:6.

547 40. Machtens DA, Willerding JM, Eschenburg S, Reubold TF. 2020. Crystal structure of the
548 metaeffector MesI (Lpg2505) from Legionella pneumophila. Biochem Bioph Res Co 527:696–701.

549 41. Hugoson E, Guliaev A, Ammunét T, Guy L. 2022. Host-adaptation in Legionellales is 1.9 Ga,
550 coincident with eukaryogenesis. Mol Biol Evol https://doi.org/10.1093/molbev/msac037.

551 42. Feeley JC, Gibson RJ, Gorman GW, Langford NC, Rasheed JK, Mackel DC, Baine WB. 1979.
552 Charcoal-yeast extract agar: primary isolation medium for Legionella pneumophila. Journal of
553 clinical microbiology 10:437 441.

554 43. Saito A, Rolfe RD, Edelstein PH, Finegold SM. 1981. Comparison of liquid growth media for
555 Legionella pneumophila. Journal of clinical microbiology 14:623 627.

556 44. Merriam JJ, Mathur R, Maxfield-Boumil R, Isberg RR. 1997. Analysis of the Legionella pneu-
557 mophila fliI gene: intracellular growth of a defined mutant defective for flagellum biosynthesis.
558 Infect Immun 65:2497–2501.

559 45. Folly-Klan M, Alix E, Stalder D, Ray P, Duarte LV, Delprato A, Zeghouf M, Antonny B,
560 Campanacci V, Roy CR, Cherfils J. 2013. A novel membrane sensor controls the localization and
561 ArfGEF activity of bacterial RalF. Plos Pathog 9:e1003747.

562 46. Geisbrecht BV, Bouyain S, Pop M. 2006. An optimized system for expression and purifica-
563 tion of secreted bacterial proteins. Protein Expres Purif 46:23–32.

564 47. Bardill JP, Miller JL, Vogel JP. 2005. IcmS-dependent translocation of SdeA into macrophages
565 by the Legionella pneumophila type IV secretion system. Mol Microbiol 56:90 103.

566 48. Blakeley BD, Chapman AM, McNaughton BR. 2012. Split-superpositive GFP reassembly is a
567 fast, efficient, and robust method for detecting protein-protein interactions in vivo. Mol Biosyst
568 8:2036 2040.

569 49. Lara-Tejero M, Sutterwala FS, Ogura Y, Grant EP, Bertin J, Coyle AJ, Flavell RA, Galán JE.
570 2006. Role of the caspase-1 inflammasome in Salmonella typhimurium pathogenesis. J Exp Med-
571 icine 203:1407 1412.

572 50. Case CL, Roy CR. 2013. Analyzing caspase-1 activation during Legionella pneumophila in-
573 fection in macrophages. Methods in molecular biology (Clifton, NJ) 954:479 491.

574 51. Arasaki K, Roy CR. 2010. Legionella pneumophila promotes functional interactions between
575 plasma membrane syntaxins and Sec22b. Traffic Cph Den 11:587–600.

576

577

578 **Tables**

579 **Table 1.** Plasmids used in this study

Name	Description	Resistance	Ref/Source
Protein production			
pT7HMT	Production of His_6-Myc fusions	Kan^R	(45)
pT7HMT::*mesI*	Production of His_6-Myc-MesI	Kan^R	(12)
pT7HMT::*mesI*$_{\Delta 10}$	Production of His_6-Myc-MesIΔ10	Kan^R	This study
pGEX6P1	Production of GST	Amp^R	GE healthcare
pGEX6P1::*sidI*	Production of GST-SidI	Amp^R	(12)
Allelic exchange			
pSR47s	Allelic exchange vector	Kan^R	(46)
pSR47s::*paraBAD*	For chromosomal integration of *araBAD-3xflag* upstream of *sidI*	Kan^R	This study
pSR47s::Δ*dotA*	For in-frame deletion of *dotA*	Kan^R	This study
Genetic complementation and cloning			
pJB1806	*Legionella* expression vector		(44)
pJB1806::*sidI* (p*sidI*)	*sidI* expression from P*tac*	Cm^R	This study
pJB1806::*sidI*$_{R453P}$ (p*sidI*$_{RP}$)	*sidI*$_{R453P}$ expression from P*tac*	Cm^R	This study
pSN85	*Legionella* vector with in-frame N-terminal *3xflag* epitope tag		(45)
pSN85::*sidI*	To generate *3xflag-sidI*	Cm^R	This study
pSN85::*mesI* (p*mesI*)	*3xflag-mesI* expression from P*tac*	Cm^R	This study
pSN85::*mesI*$_{\Delta 10}$ (p*mesI*$_{\Delta 10}$)	*3xflag-mesI*$_{\Delta 10}$ expression from P*tac*	Cm^R	This study

580
581

582

583 **Table 2**. Oligonucleotide primers used in this study

Name	Sequence[a]
Protein production	
MesIT7SalI-F	att**gtcgac**aatgataaaaggaaaacttatgccc
MesIΔ10NotI-R	att**gcggccgc**ttactcatcgtctttacc
Allelic exchange	
DotAKOSacI-F	attgtcgacgccctagctgtttcattgc
DotAKONotI-R	attgcggccgcacattctttctcacccaataac
DotAKONotI-F	att**gcggccgca**taacattcaaaaacaatata
DotAKOSalI-R	att**gagctc**ccaaaacaaaataaccagctg
SidIUTR-F	ccccc**gagctc**gagcatcaataatatcctgc
SidIUTR-R	gtagccgtcaagttgtcaaaattactttagtaaaatttttgtcatggtg
araC-pBAD-F	caccatgacaaaaattttactaaagtaattt tgacaacttgacggctacatc
araC-pBAD-R	catggtctttgtagtccat)atatctccttcttaaagttaaacaaaattatttc
3FlagSidI-F	gtttaactttaagaaggagatatatggactacaaagaccatgacg
3FlagSidI-R	ccccc**gtcgac**tgactacacccctctttattggc
Genetic complementation	
SidIBamHI-F	tta**ggatcc**ttatgactaaaatatacttattaac
SidISphI-R	att**gcatgc**tcaatcacaaattaatttttgcacatc
MesIBglII-F	tgg**agatct**ttatgataaaaggaaaacttatgc
MesISphI-R	att**gcatgc**ttataaaataattggtcgag
MesIΔ10SphI-R	att**gcatgc**ttactcatcgtctttaccagc
qRT-PCR	
sidIRT-F	atcaggcaaaccgacgtgac
sidIRT-R	ccgcaatctggtggacgaat
16SRT-F	tcagtggggaggagggttga
16SRT-R	cgctcgcaccctccgtatta
Site-directed mutagenesis	
SidIR453P-sense	ccgcaatctggtggaggaatatgaatatcaagatgagta
SidIR453P-asense	tactcatcttgatattcatattcctccaccagattgcgg

584 a-Restriction endonuclease cleavage sites are **bolded**.

585

586 **Figures**

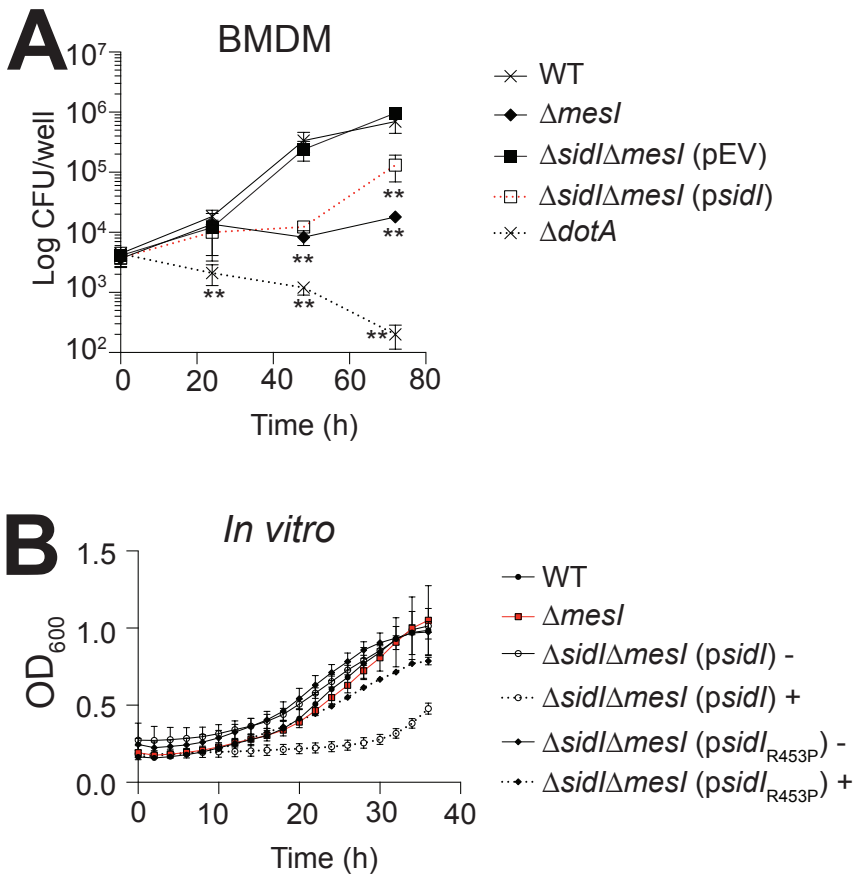

587

588

589 **Figure 1. Overexpression of *sidI* attenuates *L. pneumophila* replication. (A)** Fold replication of

590 *L. pneumophila* strains within *Nlrc4*$^{-/-}$ BMDMs over 72 h. Where indicated, infections were per-

591 formed in the presence of 1 mM IPTG. Data shown are mean ± s.d. on samples in triplicates and

592 asterisks denote statistical significance by Students' *t*-test (**P<0.01). **(B)** Optical density at 600 nm

593 (OD_{600}) of *L. pneumophila* strains grown in AYE broth. Where indicated, bacteria were grown in

594 the presence (+) or absence (-) of 1 mM IPTG. Data shown are mean ± s.d. on samples in triplicates

595 and asterisks denote statistical significance by Students' *t*-test (**P<0.01). Data shown are repre-

596 sentative of at least three independent experiments.

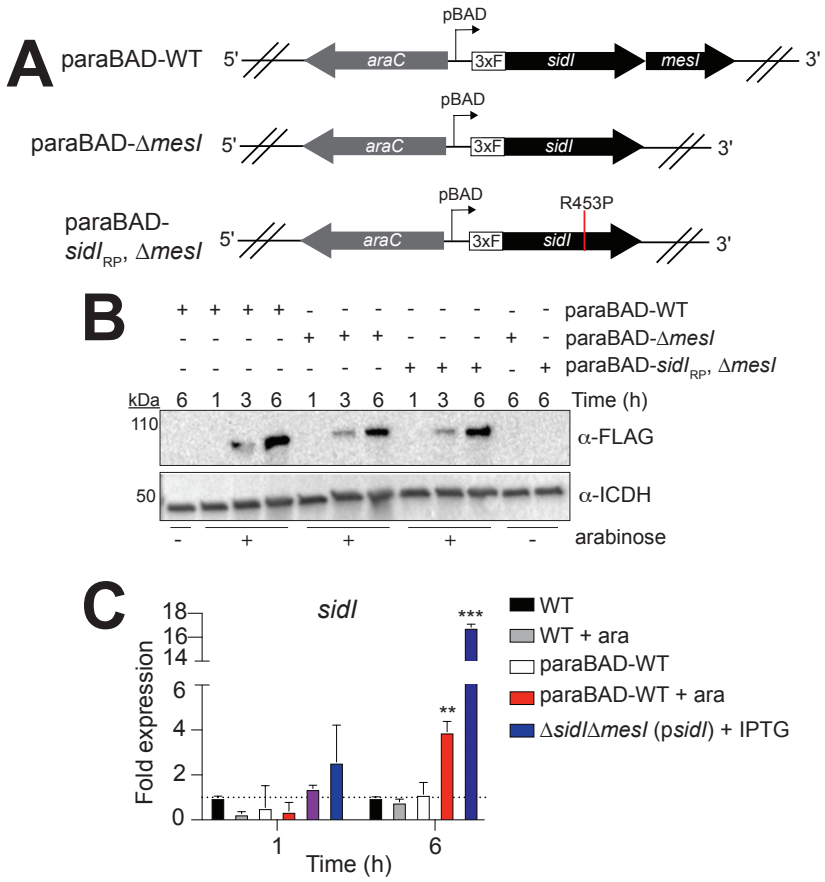

Figure 2. Establishment of a chromosomal arabinose-inducible expression system in *L. pneumophila*. (A) Schematic showing paraBAD insertion upstream of the sidI locus in the *L. pneumophila* chromosome. 3XF: In-frame *3xflag* epitope tag. **(B)** Western blot showing 3xFLAG-SidI production in the indicated paraBAD strains in the presence (+) or absence (-) of arabinose [ara; 0.6% (w/v)] after growth in AYE broth for 1, 3, or 6 h. **(C)** Quantitative RT-PCR for expression of *sidI* grown for 1 or 6 h in AYE broth. Fold expression in OD-normalized cultures (n = 3) was calculated relative to wild-type *L. pneumophila* at each time point. Asterisks denote statistical significance by Students' t-test (**P<0.01) on samples in triplicates. Data are representative of at least two independent experiments.

608

609

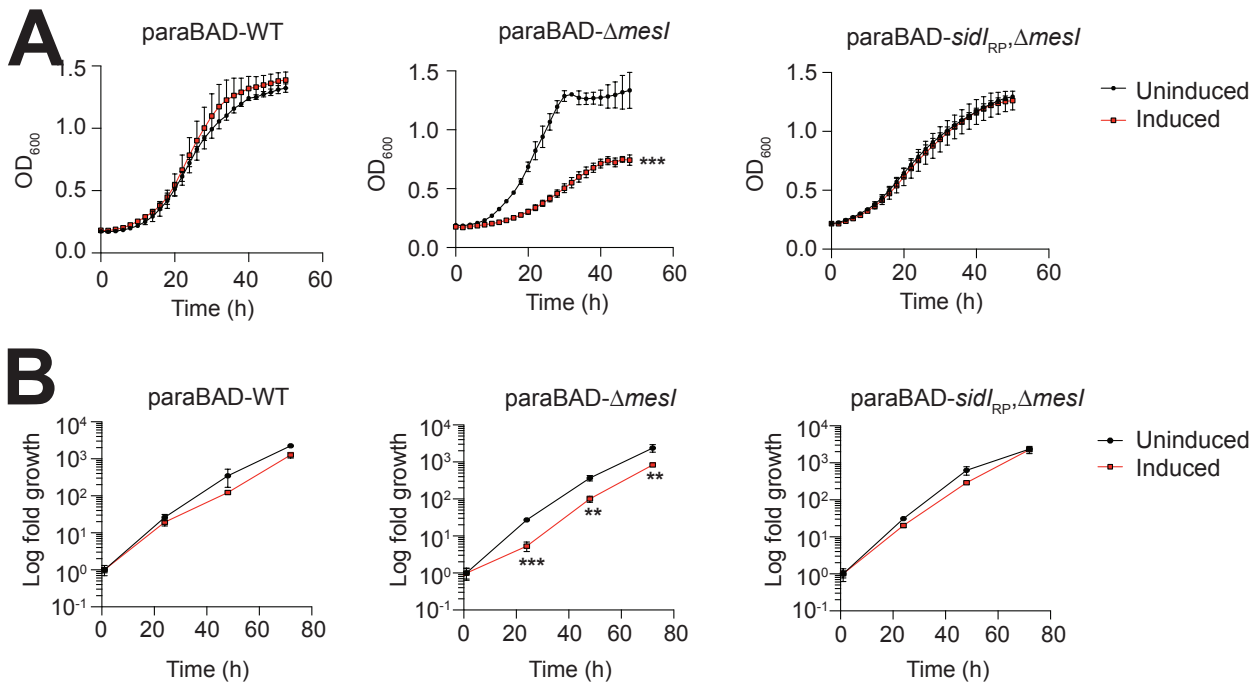

610

611

612 **Figure 3. SidI impairs *L. pneumophila* growth when uncoupled from MesI. (A)** Replication of

613 the *L. pneumophila* paraBAD strains grown in AYE broth *in vitro* under inducing [1% arabinose

614 (w/v)] or noninducing conditions. Data shown are mean ± s.d. OD600 values from samples in

615 triplicates and asterisks denote statistical significance by Students' t-test (**P<0.01). **(B)** Fold rep-

616 lication of *L. pneumophila* strains within *Nlrc4*$^{-/-}$ BMDMs under inducing [2% arabinose (w/v)] or

617 noninducing conditions. Data shown are mean ± s.d. on samples in triplicates and asterisks de-

618 note statistical significance by Students' *t*-test (**P<0.01). Data shown are representative of at least

619 three independent experiments.

620

621

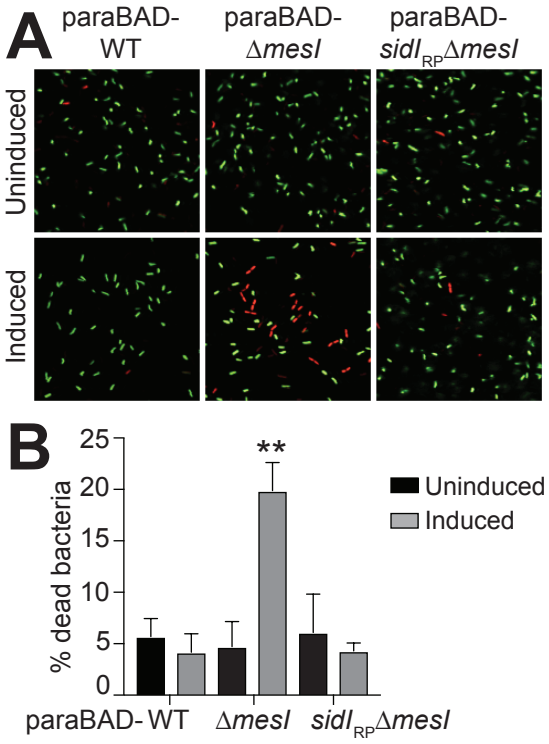

Figure 4. SidI is bactericidal in the absence of MesI. (A) Representative confocal micrographs of Live/Dead-stained *L. pneumophila* paraBAD strains grown in AYE broth under inducing [0.6% arabinose (w/v)] or noninducing conditions [SYTO9 (live; green) and propidium iodide (PI; dead; red)]. **(B)** Quantification of dead *L. pneumophila* by fluorescence microscopy following Live/Dead staining. Percent dead bacteria was calculated by dividing PI-stained cells by total cells. Data are mean ± s.d. of 650 cells scored blind and asterisks denote statistical significance by Students' *t*-test (**P<0.01). Data are representative of two independent experiments.

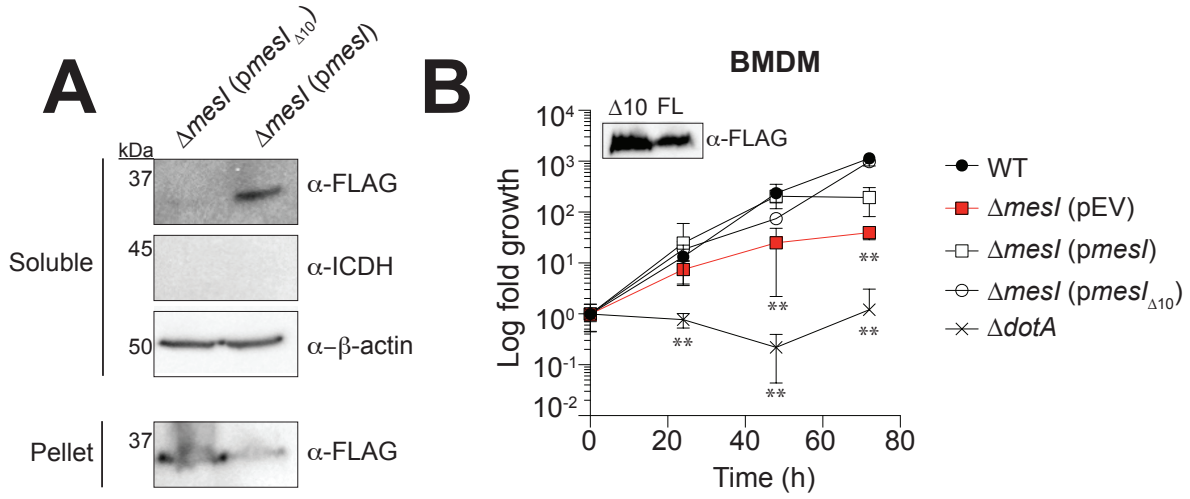

Figure 5. MesI translocation is dispensable for *L. pneumophila* intracellular replication. (A) Western blot for 3xFLAG-MesI fusion proteins in saponin-solubilized lysates of HEK293 FcγRII cells infected with antibody-opsonized *L. pneumophila* Δ*mesI* harboring p*mesI* (3xFLAG-MesI) or p*mesI*$_{\Delta 10}$ (3xFLAG-MesIΔ10). Expression of 3xFLAG-MesI fusions was confirmed by Western blot on saponin-insoluble pellets. ICDH and β-actin were used as controls for bacterial lysis and equal loading, respectively. Data are representative of three independent experiments. **(B)** Replication of *L. pneumophila* strains within *Nlrc4*$^{-/-}$ BMDMs infected at an MOI of 1. Fold growth was calculated by normalizing CFU counts to internalized bacteria at 1 h post-infection. Plasmid expression of *mesI* alleles was induced with 1 mM IPTG and confirmed by Western blot (inset). Asterisks denote statistical significance (**P<0.05) by Students' t-test on samples in triplicates. Data are representative of three independent experiments.

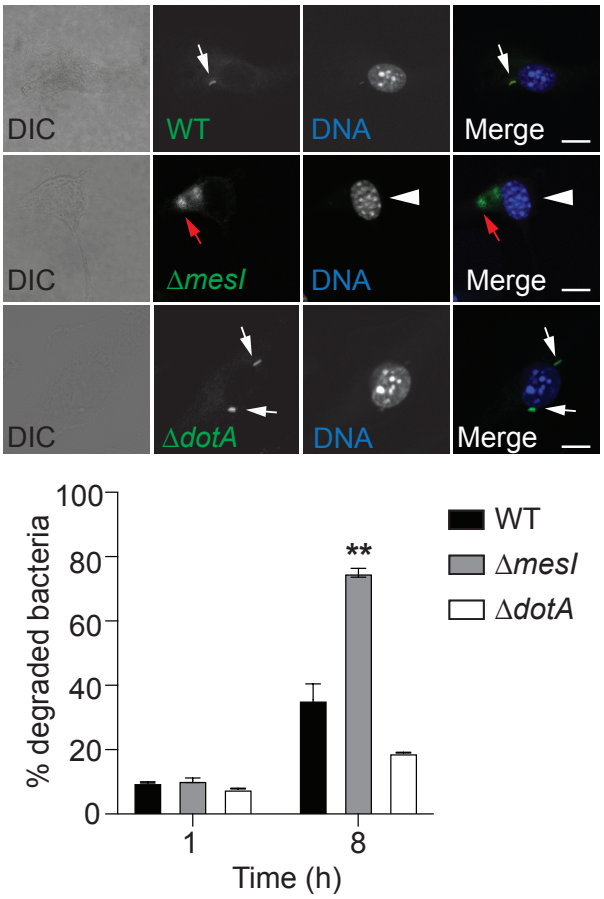

651

652 **Figure 6. MesI-deficient bacteria are efficiently degraded in host cells. (Top)** Representative
653 confocal micrographs of *Nlrc4*$^{-/-}$ BMDMs infected for 8 h (MOI of 30) with *L. pneumophila* wild-
654 type (WT), Δ*mesI*, or Δ*dotA*. Intact and degraded bacteria (green) are indicated with white and
655 red arrows, respectively. Nuclei of Δ*mesI*-infected BMDMs are indicated with white arrowhead.
656 Scale bar is 10 μm. **(Bottom)** Quantification of degraded *L. pneumophila* within *Nlrc4*$^{-/-}$ BMDMs
657 infected for 1 or 8 h at an MOI of 30. were infected with *L. pneumophila.* Percent degraded bacte-
658 ria were enumerated by blinded immunofluorescence scoring of samples in triplicates (n = 300).
659 Asterisks denote statistical significance (**P<0.01) by Students' t-test and data shown are repre-
660 sentative of two independent experiments.

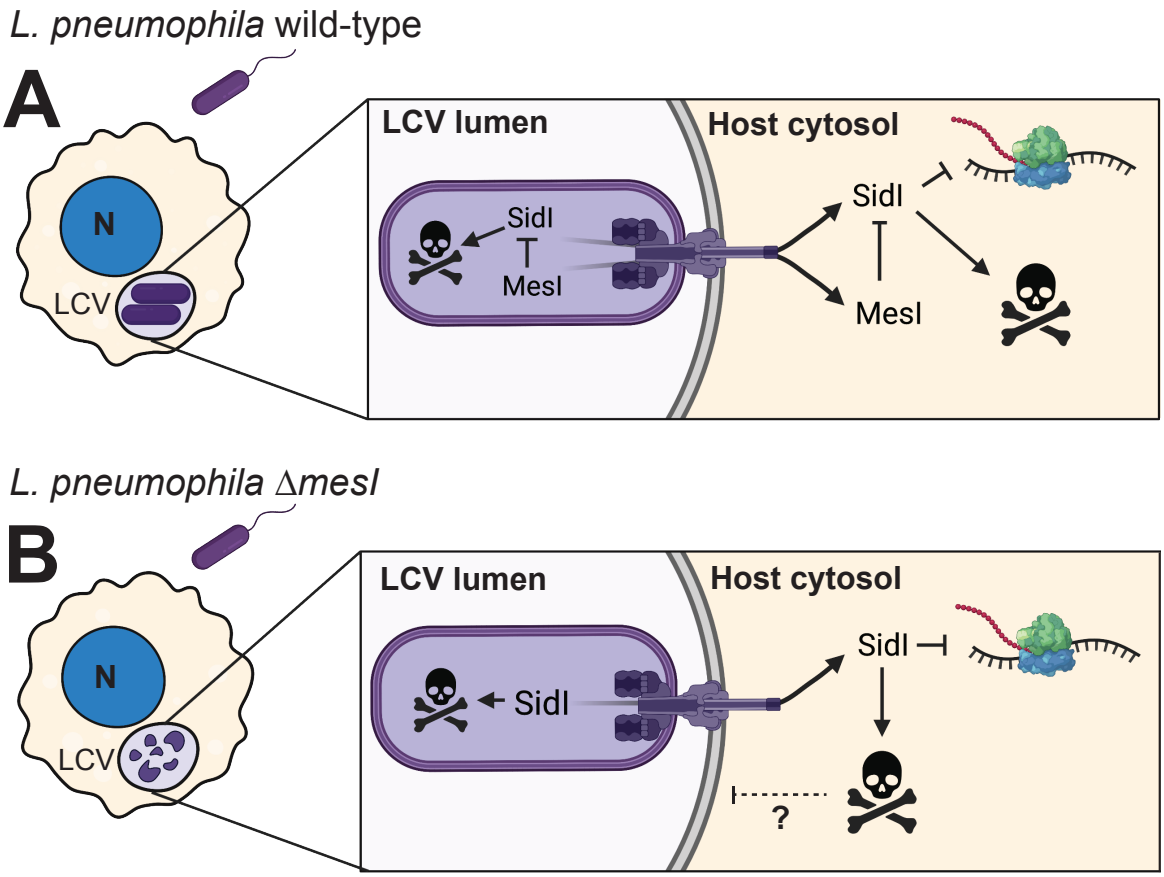

Figure 7. Model for the MesI regulatory mechanism. (A) MesI regulates SidI toxicity within host cells and the bacterium promotes replication of virulent *L. pneumophila* (purple) within host cells by regulating SidI within the bacterium and host cell. SidI inhibits eukaryotic protein synthesis and is toxic to both host cells and *L. pneumophila* in the absence of MesI. **(B)** MesI-deficient bacteria are degraded within host cells, which is likely a consequence of intrabacterial SidI toxicity. A role for SidI host cell toxicity in the *L. pneumophila ΔmesI* virulence defect is unclear (dashed line). Figure created with Biorender.com.

672 **Supplemental Figures**

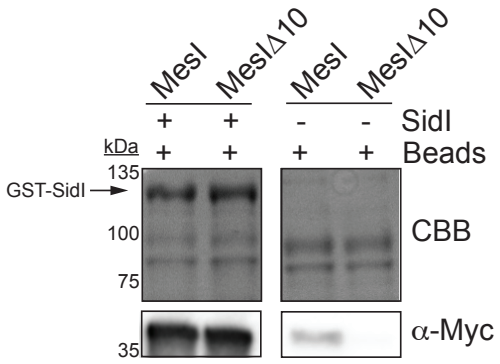

673

674 **Figure S1. MesIΔ10 binds SidI.** Glutathione agarose beads were incubated with lysates from *E.*
675 *coli* producing GST-SidI or GST (beads) and subsequently incubated with lysates from *E. coli* pro-
676 ducing His_6-Myc-MesI or -MesIΔ10. Proteins on beads were separated by SDS-PAGE and visual-
677 ized by Coomassie brilliant blue (CBB) staining or α-Myc Western blot, as indicated. Data are
678 representative of three independent experiments.

679

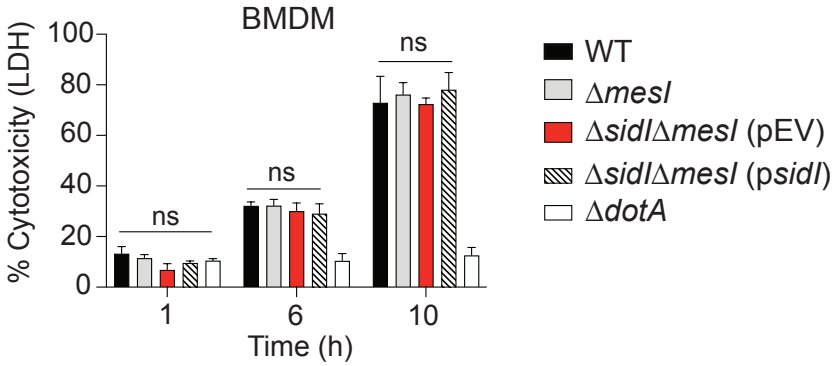

680

681 **Figure S2. Host cell death is not increased by SidI-producing *L. pneumophila*.** Lactate dehy-
682 drogenase activity in supernatants of *Nlrc4*$^{-/-}$ BMDMs infected with the indicated *L. pneumophila*
683 strains (MOI of 30) for 1, 6, or 10 h. Plasmid expression of *sidI* was induced with 1 mM IPTG.
684 Data are representative of three independent experiments and statistical analysis was per-
685 formed using Students' *t*-test (ns, not significant).